

# Multi-Task Learning for Segmentation of Male Pelvic Structures in MRI

Weixi Yi (21176856)<sup>1</sup>, Shukai Huang (21080048)<sup>2</sup>, Pengze Li (22129402)<sup>2</sup>, Fuyi Huang (22183085)<sup>1</sup>, Jiayue Chen (22091113)<sup>2</sup>, Yuhao Wu (22039936)<sup>2</sup>, and Lucien Li (22081006)<sup>2</sup>

<sup>1</sup> Department of Medical Physics and Biomedical Engineering, University College London, London, UK

<sup>2</sup> Department of Computer Science, University College London, London, UK

**Abstract.** Precise segmentation of pelvic structures surrounding the prostate is crucial for guiding biopsies and cancer radiation therapy. However, due to blurred boundaries and organ diversity, this task presents significant challenges. A multi-task learning (MTL) segmentation be approached to accurately delineate the target regions. The main concept of this approach is to draw references from structures with strong shape characteristics in the vicinity, leveraging this information to enhance the segmentation of target areas. We conducted experiments on four regions with blurred boundaries and highly variable shapes, including the transition zone, central gland, seminal vesicles, and neurovascular bundles. Experimental results demonstrated that the proposed MTL approach significantly outperforms the standalone primary tasks in accuracy, the average dice scores increased by 4.08%, 10.52%, 2.31%, and 2.57%, respectively, and are also superior to the baseline U-Net and other multi-task models.

**Key words:** Multi-task learning, MRI segmentation, Fully convolutional networks, Prostate cancer

## 1 Introduction

Globally, prostate cancer has emerged as one of the most prevalent forms of malignant tumors in men, with a continuously increasing incidence rate in recent years, posing a significant impact on public health [2]. Magnetic resonance imaging (MRI), with its advantage of no radiation exposure risk, is instrumental in the detection and management of prostate cancer [4]. Accurate segmentation of pelvic organs surrounding the prostate is vital for guiding biopsies and cancer radiotherapy [5]. However, manual annotation in this process is time-consuming, cumbersome, and requires professional expertise [18]. Therefore, a method that can automatically and reliably segment male pelvic organs in MRI is of paramount importance.

In MRI, accurate automatic segmentation of pelvic organs faces challenges such as ambiguous boundaries and diverse organ shapes [17]. To address these issues, numerous deep learning-based pelvic organ segmentation methods have been proposed in recent years. Brion et al. [1] and Nie et al. [14] employed adversarial network approaches to improve the segmentation of pelvic organs; Li et al. [10] introduced an image alignment module that fully exploits the anatomical prior knowledge between patients. However, these methods have not achieved satisfactory results in practical applications. Multi-task learning, a method for parallel processing of primary and auxiliary tasks, can improve the performance of the primary task through auxiliary tasks and is widely applied in medical image segmentation [20]. He et al. [7] and Graham et al. [6] proposed networks with segmentation as the primary task and classification as the auxiliary task, effectively enhancing the segmentation results.

This paper presents a proposed multi-task learning (MTL) network aimed at accurately segmenting male pelvic structures in MRI. The primary task employs an attention network to segment organs with ambiguous boundaries and diverse shapes, while the auxiliary task utilizes a U-Net [15] to segment the surrounding structures of the organs. The performance of the primary task is enhanced by leveraging the significant geometric correlations between the organ and its surrounding structures [19]. We conducted experiments on four regions characterized by blurred boundaries and highly variable shapes, including the transition zone, central gland, seminal vesicles, and neurovascular bundles [10]. Experimental results demonstrate that the proposed MTL method achieves a significant improvement in accuracy compared to a single primary task and outperforms baseline U-Net and other multi-task models.

## 2 Methods

In this section, we elaborate on the proposed MTL method for male pelvic structure segmentation. The MTL, based on AMTA-U-Net [19] and illustrated in 1, takes 3D MRI as input. The network is composed of two components: the main task and the auxiliary task. The main task part adopts an attention network composed of multiple cascaded attention modules for the segmentation of the target area. The auxiliary task part employs a network with a U-Net architecture for the segmentation of the surrounding tissues of the target area.

The auxiliary utilizes U-Net, a traditionally efficient and well-established fully convolutional network (FCN) architecture designed for medical image segmentation, including an encoder and a decoder. The encoder is primarily responsible for extracting image features, while the decoder maps the features back to the original image space, generating pixel-level segmentation results. As the input image propagates through the network, we can obtain the gradually increasing feature maps of the surrounding tissue structure, providing support for the main task part to segment the target area.

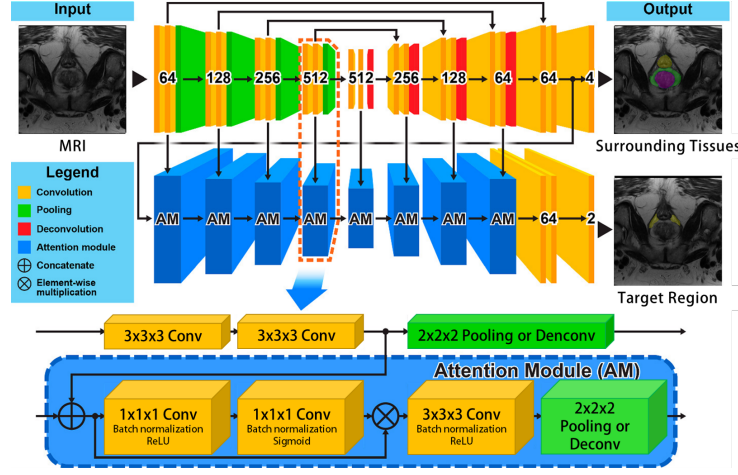


Fig. 1. Illustration of MTL model

The boundaries of the target area in the male pelvis largely depend on the shape of the surrounding tissues. Therefore, the features of the surrounding tissue segmentation can serve as a reference for the target area segmentation. In the main task part, we design an attention network based on the attention mechanism [11], which receives the surrounding tissue features from the auxiliary task part simultaneously. The attention network comprises multiple attention modules, aiming to focus more on the target area features. Each attention module is connected to the corresponding U-Net convolution block, utilizing the structural information of the target area and surrounding tissues to enhance the segmentation quality.

We adopt the Dice Loss [12] as our loss function:

$$L_{dice} = 1 - \frac{2|X \cap Y|}{|X| + |Y|} \quad (1)$$

Where  $X$  and  $Y$  are the predicted and ground truth binary masks, respectively.

### 3 Experiments

In this experiment, we employ a cross-institutional male pelvic structure dataset [9], which encompasses 589 T2-weighted images from seven research projects, involving eight different tissue structures, including the bladder, skeleton, neurovascular bundle, obturator internus muscle, regions, rectum, seminal vesicles, transition zone, and peripheral zone. We randomly allocate 80% of the dataset (a total of 471 images) as the training set, with the remaining portion (118 images) serving as the test set. Considering that the data originates from various

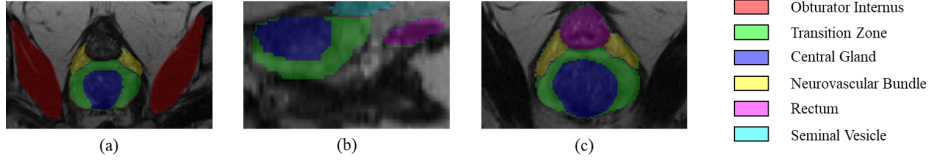


**Fig. 2.** Illustration of four regions with ambiguous boundaries and highly variable shapes, along with their surrounding tissues, which include: (a) the transition zone and central gland, as well as their surrounding tissues, (b) the seminal vesicle and its surrounding tissues, and (c) the neurovascular bundle and its surrounding tissues.

scanners and features diverse fields of view and voxel sizes, we normalize the data, enhance the contrast using adaptive histogram equalization techniques, and finally resample it to (256,256,32).

We use the Adam optimizer [8] for training, setting the initial learning rate to  $lr=2e-4$ . The network implementation is based on publicly available frameworks: PyTorch 2.0.0 and Python 3.10.3. Training and testing are conducted on a Linux server equipped with an NVIDIA GeForce GTX TITAN X GPU.

We conduct experiments on four areas characterized by blurred boundaries and highly variable shapes, including the transition zone, central gland, seminal vesicle, and neurovascular bundle. The relationship diagram of these four areas and their surrounding structures is shown in Figure 2. Based on the association between the target area and its surrounding tissues, as well as relevant anatomical knowledge, we set the main segmentation tasks and auxiliary segmentation tasks for the four experimental groups as follows: 1) Main task: transition zone. Auxiliary tasks: obturator internus, central gland, and neurovascular bundle. 2) Main task: central gland. Auxiliary tasks: obturator internus, transition zone, and neurovascular bundle. 3) Main task: seminal vesicle. Auxiliary tasks: transition zone, central gland, and rectum. 4) Main task: neurovascular bundle. Auxiliary tasks: transition zone, central gland, and rectum. In each experiment, we compare the MTL approach with the approach that only performs the main task to evaluate the improvement effect of the auxiliary tasks on the main task, while also comparing them with the baseline U-Net and the advanced multi-task learning network proposed by Nguyen et al.[13].

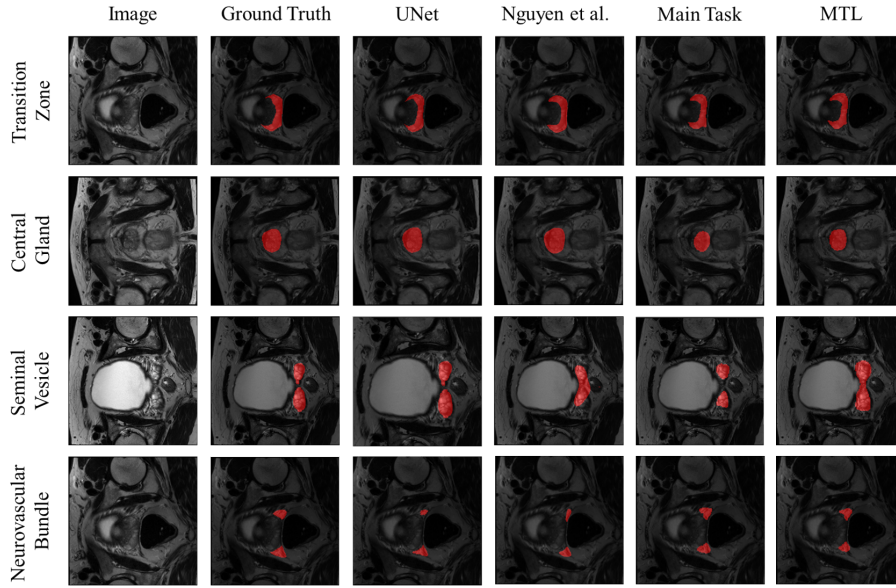
We employ the Dice coefficient to assess the accuracy of the image segmentation models, as the Dice coefficient is capable of measuring the overlap between predictions and ground truth.

## 4 Results

After evaluating the model using the test set, the experimental results are shown in Table 1, and the predictions are shown in Figure 3. When conducting exper-

**Table 1.** Experiment results of different methods

Methods	Transition Zone	Central Gland	Seminal Vesicles	Neurovascular Bundles
U-Net	0.5866	0.7252	0.4799	0.4326
Nguyen et al.	0.5624	0.7569	0.4821	0.5674
Main Task	0.6323	0.7351	0.5282	0.5691
MTL	<b>0.6581</b>	<b>0.8124</b>	<b>0.5404</b>	<b>0.5837</b>

**Fig. 3.** Illustration of predictions

iments on the four parts: transition zone, central gland, seminal vesicles, and neurovascular bundles, using the segmentation of surrounding tissues as an auxiliary task, the average Dice scores increased by 4.08%, 10.52%, 2.31%, and 2.57%, respectively. These results suggest that the structural information of the surrounding tissues of the target regions contributes to improved segmentation accuracy. Furthermore, compared with the baseline U-Net and the state-of-the-art multi-task learning methods, the MTL achieved the highest Dice scores for all four regions, with values of 0.6581, 0.8124, 0.5404, and 0.5837, respectively. This indicates that the MTL provides exceptional segmentation accuracy for male pelvic structures and holds potential for clinical applications to aid in diagnosis and treatment. In addition, the Main Task method outperforms both the baseline U-Net and the state-of-the-art multi-task learning methods in most regions, demonstrating the effectiveness of the attention module in focusing on target areas and enhancing segmentation performance.

However, there are some limitations to using the MTL: First, it demands high-quality datasets with annotated information for both the target regions and their surrounding tissues. Noise or artifacts in the images may also impact the segmentation accuracy. Second, the complexity of the model may lead to increased computational requirements and longer training times. Moreover, during the training process, as the main and auxiliary tasks share some network parameters, an inappropriate design of the main and auxiliary tasks may hinder the network’s ability to effectively learn features, resulting in the loss function not converging to a reasonable value.

Accurate segmentation of various regions of the prostate gland, including transition zone, central gland, seminal vesicles, and neurovascular bundles, carries substantial clinical value. The transition zone is where Benign Prostatic Hyperplasia (BPH) often develops[16]. Precise transition zone segmentation assists in diagnosing and treating BPH. The central gland is the critical area where prostate cancer can develop. Segmentation of the central gland plays a pivotal role in detecting and localizing prostate cancer[3]. The seminal vesicles, which produce a significant portion of the seminal fluid, can also be involved in prostate cancer, impacting prognosis and treatment. Neurovascular bundles is responsible for erectile function and accurate neurovascular bundles segmentation helps avoid side effects of prostate cancer treatment. In conclusion, accurate segmentation of these prostate regions can significantly aid in the diagnosis, staging, and treatment of various prostate diseases, such as BPH and prostate cancer, thereby improving the success rate of surgery and mitigating side effects.

## 5 Discussion and Conclusion

In summary, we propose an innovative MTL method for addressing the challenging problem of segmenting regions with ambiguous boundaries and diverse shapes in male pelvic structures in MRI. The MTL method consists of a primary task and auxiliary tasks, where the auxiliary tasks employ a U-Net structure to segment the tissues surrounding the target region, while the primary task is based on attention modules and shares the feature maps of the surrounding tissues with the auxiliary tasks to improve the segmentation accuracy of the target region. The effectiveness of the proposed strategy is validated through extensive experiments on a multi-institutional male pelvic dataset containing 589 MRI images. However, this method also has limitations, mainly reflected in the high requirements for multi-label datasets and the design of primary and auxiliary tasks. In the future, we will continue to explore the application of multi-task learning in more disease domains.

## References

1. Brion, E., Léger, J., Barragán-Montero, A.M., Meert, N., Lee, J.A., Macq, B.: Domain adversarial networks and intensity-based data augmentation for male pelvic organ segmentation in cone beam ct. *Computers in Biology and Medicine* **131**, 104269 (2021)
2. De Vente, C., Vos, P., Hosseinzadeh, M., Pluim, J., Veta, M.: Deep learning regression for prostate cancer detection and grading in bi-parametric mri. *IEEE Transactions on Biomedical Engineering* **68**(2), 374–383 (2020)
3. Engelbrecht, M.R., Huisman, H.J., Laheij, R.J., Jager, G.J., van Leenders, G.J., Hulsbergen-Van De Kaa, C.A., de la Rosette, J.J., Blickman, J.G., Barentsz, J.O.: Discrimination of prostate cancer from normal peripheral zone and central gland tissue by using dynamic contrast-enhanced mr imaging. *Radiology* **229**(1), 248–254 (2003)
4. Feng, Z., Nie, D., Wang, L., Shen, D.: Semi-supervised learning for pelvic mr image segmentation based on multi-task residual fully convolutional networks. In: 2018 IEEE 15th International Symposium on Biomedical Imaging (ISBI 2018). pp. 885–888. IEEE (2018)
5. Fu, Y., Lei, Y., Wang, T., Tian, S., Patel, P., Jani, A.B., Curran, W.J., Liu, T., Yang, X.: Pelvic multi-organ segmentation on cone-beam ct for prostate adaptive radiotherapy. *Medical physics* **47**(8), 3415–3422 (2020)
6. Graham, S., Vu, Q.D., Jahanifar, M., Raza, S.E.A., Minhas, F., Snead, D., Rajpoot, N.: One model is all you need: multi-task learning enables simultaneous histology image segmentation and classification. *Medical Image Analysis* **83**, 102685 (2023)
7. He, T., Hu, J., Song, Y., Guo, J., Yi, Z.: Multi-task learning for the segmentation of organs at risk with label dependence. *Medical Image Analysis* **61**, 101666 (2020)
8. Kingma, D.P., Ba, J.: Adam: A method for stochastic optimization. *arXiv preprint arXiv:1412.6980* (2014)
9. Li, Y., Fu, Y., Gayo, I.J., Yang, Q., Min, Z., Saeed, S.U., Yan, W., Wang, Y., Noble, J.A., Emberton, M., Clarkson, M.J., Huisman, H., Barratt, D.C., Prisacariu, V.A., Hu, Y.: Cross-institution male pelvic structures (Sep 2022)
10. Li, Y., Fu, Y., Yang, Q., Min, Z., Yan, W., Huisman, H., Barratt, D., Prisacariu, V.A., Hu, Y.: Few-shot image segmentation for cross-institution male pelvic organs using registration-assisted prototypical learning. In: 2022 IEEE 19th International Symposium on Biomedical Imaging (ISBI). pp. 1–5 (2022)
11. Liu, S., Johns, E., Davison, A.J.: End-to-end multi-task learning with attention. In: *Proceedings of the IEEE/CVF conference on computer vision and pattern recognition*. pp. 1871–1880 (2019)
12. Milletari, F., Navab, N., Ahmadi, S.A.: V-net: Fully convolutional neural networks for volumetric medical image segmentation. In: 2016 fourth international conference on 3D vision (3DV). pp. 565–571. Ieee (2016)
13. Nguyen, H.H., Fang, F., Yamagishi, J., Echizen, I.: Multi-task learning for detecting and segmenting manipulated facial images and videos. In: 2019 IEEE 10th International Conference on Biometrics Theory, Applications and Systems (BTAS). pp. 1–8. IEEE (2019)
14. Nie, D., Wang, L., Gao, Y., Lian, J., Shen, D.: Strainet: Spatially varying stochastic residual adversarial networks for mri pelvic organ segmentation. *IEEE Transactions on Neural Networks and Learning Systems* **30**(5), 1552–1564 (2019)
15. Ronneberger, O., Fischer, P., Brox, T.: U-net: Convolutional networks for biomedical image segmentation. In: *Medical Image Computing and Computer-Assisted*

- Intervention–MICCAI 2015: 18th International Conference, Munich, Germany, October 5–9, 2015, Proceedings, Part III 18. pp. 234–241. Springer (2015)
16. Thorpe, A., Neal, D.: Benign prostatic hyperplasia. *The Lancet* **361**(9366), 1359–1367 (2003)
  17. Wang, S., He, K., Nie, D., Zhou, S., Gao, Y., Shen, D.: Ct male pelvic organ segmentation using fully convolutional networks with boundary sensitive representation. *Medical image analysis* **54**, 168–178 (2019)
  18. Wang, S., Wang, Q., Shao, Y., Qu, L., Lian, C., Lian, J., Shen, D.: Iterative label denoising network: Segmenting male pelvic organs in ct from 3d bounding box annotations. *IEEE Transactions on Biomedical Engineering* **67**(10), 2710–2720 (2020)
  19. Xu, X., Lian, C., Wang, S., Wang, A., Royce, T., Chen, R., Lian, J., Shen, D.: Asymmetrical multi-task attention u-net for the segmentation of prostate bed in ct image. In: *Medical Image Computing and Computer Assisted Intervention–MICCAI 2020: 23rd International Conference, Lima, Peru, October 4–8, 2020, Proceedings, Part IV* 23. pp. 470–479. Springer (2020)
  20. Zhou, Y., Chen, H., Li, Y., Liu, Q., Xu, X., Wang, S., Yap, P.T., Shen, D.: Multi-task learning for segmentation and classification of tumors in 3d automated breast ultrasound images. *Medical Image Analysis* **70**, 101918 (2021)